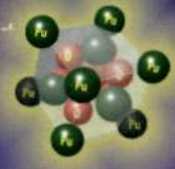
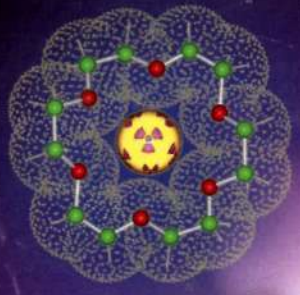


ПН
I-65

Inorganic Chemistry

including bioinorganic chemistry

April 1, 2013
Volume 52, Number 7
pubs.acs.org/IC



Forum on Aspects of Inorganic Chemistry Related to Nuclear Energy



57 La lanthanum 138.9	58 Ce cerium 140.1	59 Pr praseodymium 140.9	60 Nd neodymium 144.2	61 Pm promethium (145)	62 Sm samarium 150.4	63 Eu europium 152.0	64 Gd gadolinium 157.2	65 Tb terbium 158.9	66 Dy dysprosium 162.5	67 Ho holmium 164.9	68 Er erbium 167.3	69 Tm thulium 168.9	70 Yb ytterbium 173.0	71 Lu lutetium 175.0
89 Ac actinium (227)	90 Th thorium 232	91 Pa protactinium 231	92 U uranium 238	93 Np neptunium (237)	94 Pu plutonium (244)	95 Am americium (243)	96 Cm curium (247)	97 Bk berkelium (247)	98 Cf californium (251)	99 Es einsteinium (252)	100 Fm fermium (257)	101 Md mendelevium (258)	102 No nobelium (259)	103 Lr lawrencium (262)

ON THE COVER: The cover highlights some topics featured in this Forum on Aspects of Inorganic Chemistry Related to Nuclear Energy. Articles highlight fundamental as well as application-driven efforts of researchers working in the field. The Forum is introduced in the Preface by John C. Gordon (guest editor) and Ken Czerwinski and Lynn Francesconi (co-guest editors), p 3405.

Forum on Aspects of Inorganic Chemistry Related to Nuclear Energy

Forum Articles

3405

[dx.doi.org/10.1021/ic4006136](https://doi.org/10.1021/ic4006136)

Preface: Forum on Aspects of Inorganic Chemistry Related to Nuclear Energy

John C. Gordon,* Kenneth Czerwinski, and Lynn Francesconi

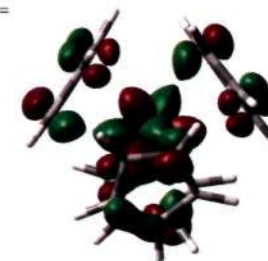
3407

[dx.doi.org/10.1021/ic3006025](https://doi.org/10.1021/ic3006025)

Does Covalency Increase or Decrease across the Actinide Series? Implications for Minor Actinide Partitioning

Nikolas Kaltsoyannis

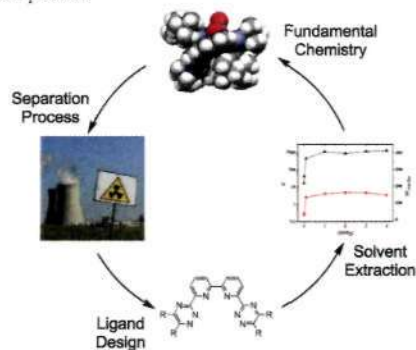
A comparison of topological analyses of the electron densities in $AnCp_3$ and $AnCp_4$ ($An = Th-Cm$) with more traditional computational measures of the covalency leads to an unexpected answer to the title question, the implications of which for minor actinide partitioning are discussed.



Use of Soft Heterocyclic N-Donor Ligands To Separate Actinides and Lanthanides

Michael J. Hudson,* Laurence M. Harwood, Dominic M. Laventine, and Frank W. Lewis

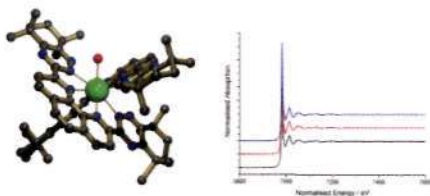
The removal of the radiotoxic minor actinides from used nuclear fuel is foreseen as a key step toward reducing geological storage times of nuclear waste and increasing the public acceptance of nuclear energy. The SANEX process is proposed to carry out this selective separation by solvent extraction. Recent efforts to develop reagents capable of separating the radioactive minor actinides from lanthanides are discussed in this review, together with advances in our understanding of the underlying chemistry involved in this separation process.



Lanthanide Speciation in Potential SANEX and GANEX Actinide/Lanthanide Separations Using Tetra-N-Donor Extractants

Daniel M. Whittaker,* Tamara L. Griffiths, Madeleine Helliwell, Adam N. Swinburne, Louise S. Natrajan, Frank W. Lewis, Laurence M. Harwood, Stephen A. Parry, and Clint A. Sharrad*

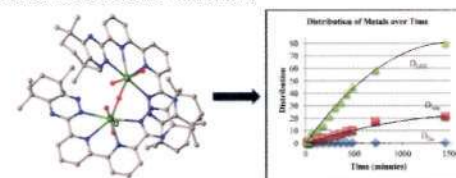
A series of lanthanide(III) complexes with the N-donor extractant molecules, CyMe₂-BTBP and CyMe₄BTPhen, which exhibit the potential for the separation of minor actinides from lanthanides in the management of spent nuclear fuel, have been prepared and characterized in solution and solid states. This information is used to assess the lanthanide(III) speciation obtained when extracted into the organic phase in liquid–liquid separation conditions, probed by X-ray absorption spectroscopy.



Coordination Chemistry with f-Element Complexes for an Improved Understanding of Factors That Contribute to Extraction Selectivity

Anne E. V. Gorden,* Michael A. DeVore II, and Branson A. Maynard

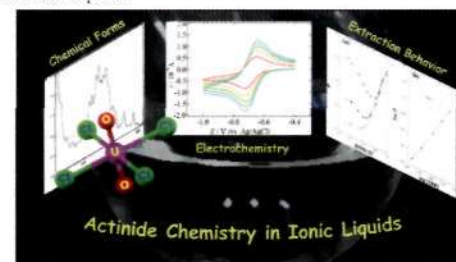
Understanding coordination leads to more selective extractions.



Actinide Chemistry in Ionic Liquids

Koichiro Takao, Thomas James Bell, and Yasuhisa Ikeda*

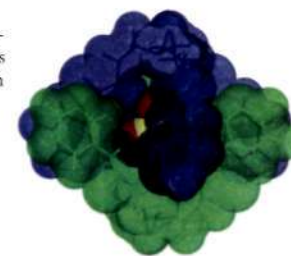
This Forum Article provides an overview of the reported studies on the actinide chemistry in ionic liquids with a particular focus on several fundamental chemical aspects.



A Case for Molecular Recognition in Nuclear Separations: Sulfate Separation from Nuclear Wastes

Bruce A. Moyer,* Radu Custelcean, Benjamin P. Hay, Jonathan L. Sessler, Kristin Bowman-James, Victor W. Day, and Sung-Ok Kang

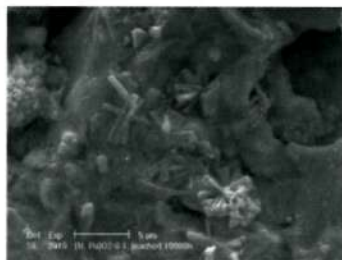
The case for molecular-recognition approaches for sulfate removal from radioactive wastes is presented. Selective sulfate separation can be achieved via the use of anion-sequestering systems using either liquid–liquid extraction or crystallization. Receptors that have been shown to have promising affinity for sulfate, either in extraction or in crystallization experiments, include hexaurea tripods, tetraamide macrocycles, cyclo[8]pyrroles, calixpyrroles, and self-assembled urea-lined cages.



3491  dx.doi.org/10.1021/ic302012c

Reducing Uncertainties Affecting the Assessment of the Long-Term Corrosion Behavior of Spent Nuclear Fuel
 Thomas Fanghänel, Vincenzo V. Rondinella,* Jean-Paul Glatz, Thierry Wiss, Detlef H. Wegen, Thomas Gouder, Paul Carbol, Daniel Serrano-Purroy, and Dimitrios Papaioannou

Corrosion products on the surface of (U,Pu)O₂ after ~400 days of leaching in groundwater are shown.

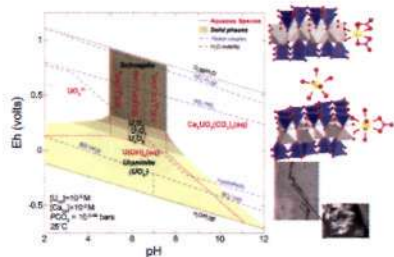


3510  dx.doi.org/10.1021/ic301686d

Environmental Speciation of Actinides

Kate Maher,* John R. Bargar, and Gordon E. Brown Jr.

This review of actinide speciation in the environment highlights the development of mechanistic information derived from a variety of spectroscopic techniques and the application of such knowledge to quantify and predict microscopic to macroscopic transport behaviors. We also provide an overview of uranium or plutonium speciation and remediation strategies across a range of contaminated sites (e.g., Hanford, WA; Oak Ridge, TN; Rifle, CO; Fernald, OH; Fry Canyon, UT; and Rocky Flats, CO).

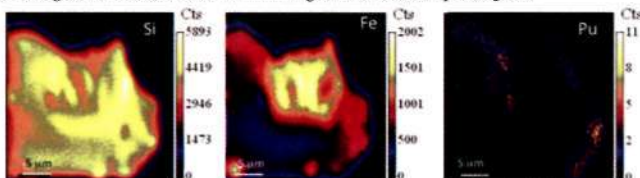


3533  dx.doi.org/10.1021/ic3018908

Plutonium Transport in the Environment

Annie B. Kersting*

Recent laboratory and field studies show long-distance transport of plutonium (Pu) in several different hydrogeological environments, which is a key concern for the development of safe long-term, high-level waste storage. This review summarizes the current understanding of relevant conditions and processes controlling the behavior of Pu in the environment, gaps in our scientific knowledge, and future research needs. A NanoSIMS image of contaminated Hanford vadose zone sediments collected 20 m below the ground surface shows Pu rimming an iron-coated quartz grain.

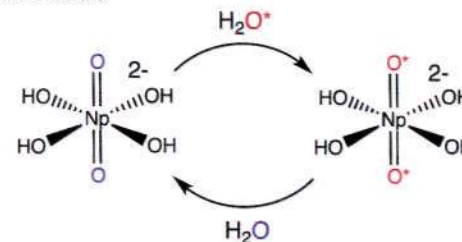



3547  dx.doi.org/10.1021/ic3020139

Chemical Speciation of Neptunium(VI) under Strongly Alkaline Conditions. Structure, Composition, and Oxo Ligand Exchange

David L. Clark,* Steven D. Conradson, Robert J. Donohoe, Pamela L. Gordon, D. Webster Keogh, Phillip D. Palmer, Brian L. Scott, and C. Drew Tait

The combination of EXAFS and Raman data suggests that NpO₂(OH)₄²⁻ is the dominant species in a 2.5M alkaline solution, with a small amount of NpO₂(OH)₅³⁻ present at higher alkalinity. Isotopic labeling studies with ¹⁸O reveal a facile exchange of neptunylxo ligands with the water solvent.

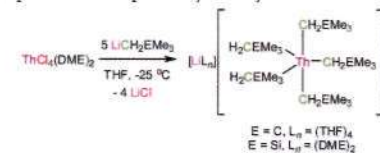


3556  dx.doi.org/10.1021/ic300867m

In Pursuit of Homoleptic Actinide Alkyl Complexes

Lani A. Seaman, Justin R. Walensky,* Guang Wu, and Trevor W. Hayton*

Treatment of ThCl₄(DME)₂ with 5 equiv of LiCH₂Bu or LiCH₂SiMe₃ at -25 °C in THF affords [Li(THF)₄][Th(CH₂Bu)₅] (1) and [Li(DME)₂][Th(CH₂SiMe₃)₅] (2), respectively, in moderate yields. Similarly, treatment of ThCl₄(DME)₂ with 6 equiv of K(CH₂Ph) produces [K(THF)₂][Th(CH₂Ph)₆] (3), in good yield. Complexes 1 and 3 were both structurally characterized and their electronic properties were explored by density functional theory.

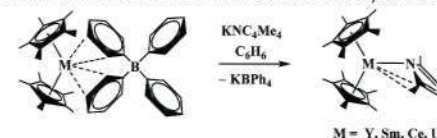


3565  dx.doi.org/10.1021/ic300905r

Density Functional Theory and X-ray Analysis of the Structural Variability in η⁵,η⁵,η¹-Tris(ring) Rare Earth/Actinide Tetramethylpyrrolyl Complexes, (C₅Me₅)₂M(NC₄Me₄)

Christopher L. Webster, Jefferson E. Bates, Ming Fang, Joseph W. Ziller, Filipp Furche, and William J. Evans*

The structures of the 4d, 4f, and 5f metal complexes (C₅Me₅)₂M(NC₄Me₄) (M = Y, Sm, Ce, U) reveal that the (NC₄Me₄)⁻ anion displays agostic interactions with the [(C₅Me₅)₂M]⁺ framework that can be modeled by density functional theory calculations. However, large structural variations are found even between two crystals isolated from the same mother liquor.



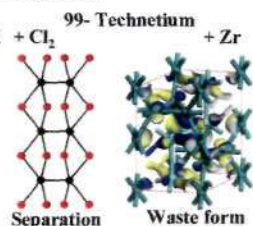
3573

Technetium Chemistry in the Fuel Cycle: Combining Basic and Applied Studies

Frederic Poineau, Edward Mausolf, Gordon D. Jarvinen, Alfred P. Sattelberger, and Kenneth R. Czerwinski*

Technetium halides, technetium–zirconium alloys, and low-valent technetium complexes demonstrate trends with structure, coordination number, and speciation that can be utilized in the nuclear fuel cycle.

dx.doi.org/10.1021/ic3016468

**Communications**

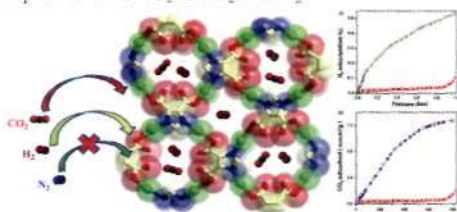
3579

Synthesis, Structure, and H₂/CO₂ Adsorption in a Three-Dimensional 4-Connected Triorganotin Coordination Polymer with a sqc Topology

Vadapalli Chandrasekhar,* Chandrajeet Mohapatra, Rahul Banerjee,* and Arijit Mallick

A 3-fold parallel interpenetrated 3D coordination polymer containing triorganotin units has been constructed with 4-connected sqc topology, which possesses three types of 1D microchannels along its crystallographic *a* axis. Moreover, this framework shows selective gas sorption for both CO₂ and H₂ over N₂.

dx.doi.org/10.1021/ic302528b



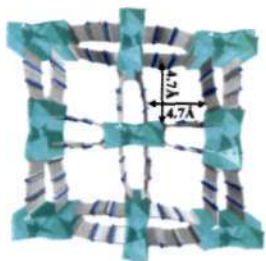
3582

Europium Pyrimidine-4,6-dicarboxylate Framework with a Single-Crystal-to-Single-Crystal Transition and a Reversible Dehydration/Rehydration Process

Hao-Ling Sun,* Dan-Dan Yin, Qi Chen, and Zhenqiang Wang*

In this paper, a novel three-dimensional (3D) porous lanthanide–organic framework (LnOF), Eu₂(μ₄-pmdc)₂(OH)₂·3H₂O (**1**), which is stable up to 400 °C, has been hydrothermally synthesized and characterized. It shows intriguing single-crystal-to-single-crystal transformation and reversible dehydration/rehydration phenomenon upon removal and rebinding of the lattice water molecules, which is supported by single-crystal X-ray diffraction, powder X-ray diffraction, and photoluminescence data. Furthermore, compared with the original sample **1**, the dehydrated phase **2** has modified photoluminescent behavior with a longer lifetime and emission quantum yield. These results suggest that our LnOF system represents a promising candidate for structural probing and fluoroimmunoassays.

dx.doi.org/10.1021/ic302556r



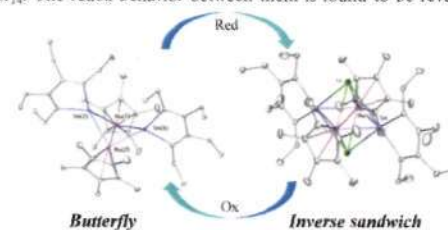
3585

Unexpected Formation of Ru₂Sn₂ Bicyclic Four-Membered Ring Complexes with Butterfly and Inverse-Sandwich Structures

Takuya Kuwabara, Masaichi Saito,* Jing-Dong Guo, and Shigeru Nagase

Novel bicyclic Ru₂Sn₂ complexes with butterfly and inverse-sandwich structures were obtained from reactions of dithiostannole with [Cp*RuCl]₄. The redox behavior between them is found to be reversible.

dx.doi.org/10.1021/ic302782n



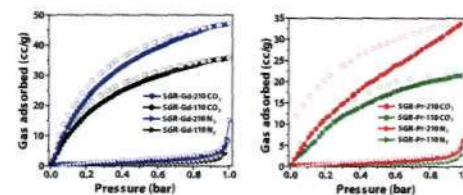
3588

Azide-Functionalized Lanthanide-Based Metal–Organic Frameworks Showing Selective CO₂ Gas Adsorption and Postsynthetic Cavity Expansion

Sumi Ganguly, Pradip Pachfule, Sukhen Bala, Arijit Goswami, Sudeshna Bhattacharya, and Raju Mondal*

We report herein two lanthanide-based metal–organic frameworks (MOFs) with azide groups as immobilized functional groups. Both compounds show selective CO₂ gas adsorption over N₂. Furthermore, this work also demonstrates that these MOFs can be used for *postsynthetic cavity expansion*, a novel method of enhancing the porosity by selective thermolysis of azide groups.

dx.doi.org/10.1021/ic302823r



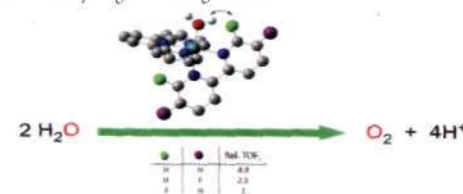
3591

Mononuclear Ruthenium–Water Oxidation Catalysts: Discerning between Electronic and Hydrogen-Bonding Effects

Somnath Maji, Isidoro López, Fernando Bozoglian, J. Benet-Buchholz, and Antoni Llobet*

New ruthenium–water complexes containing fluorine-substituted bipyridine have been prepared and thoroughly characterized. Their catalytic performance with regard to the oxidation of water to dioxygen changes dramatically and is rationalized in terms of electronic and hydrogen-bonding effects.

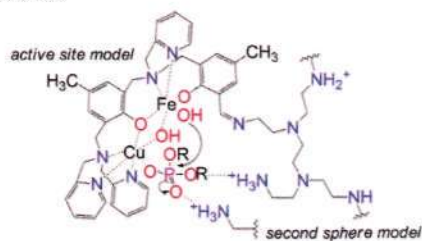
dx.doi.org/10.1021/ic3028176



Second-Coordination-Sphere Effects Increase the Catalytic Efficiency of an Extended Model for Fe^{III}M^I Purple Acid Phosphatases

Bernardo de Souza,* Gabriel L. Kreft, Tiago Bortolotto, Hernán Terenzi, Adailton J. Bortoluzzi, Eduardo E. Castellano, Rosely A. Peralta, Josiel B. Domingos, and Ademir Neves*

Herein we describe the synthesis of a new heterodinuclear Fe^{III}Cu^I model complex for the active site of purple acid phosphatases and its binding to a polyamine chain, a model for the amino acid residues around the active site. The properties of these systems and their catalytic activity in the hydrolysis of bis(2,4-dinitrophenyl)phosphate are compared, and conclusions regarding the effects of the second coordination sphere are drawn. The positive effect of the polymeric chain on DNA hydrolysis is also described and discussed.

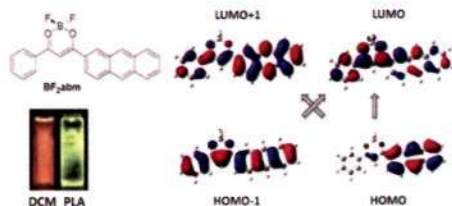


Articles

Aromatic Difluoroboron β -Diketonate Complexes: Effects of π -Conjugation and Media on Optical Properties

Songpan Xu, Ruffin E. Evans, Tiandong Liu, Guoqing Zhang, J. N. Demas, Carl O. Trindle, and Cassandra L. Fraser*

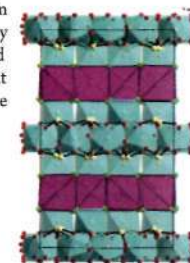
Aromatic difluoroboron β -diketonate complexes were synthesized and their photophysical properties were investigated in CH₂Cl₂ and poly(lactic acid) (PLA). Small symmetrical dyes exhibit π - π^* transitions and comparable luminescence in CH₂Cl₂ and PLA, but dyes with larger arene rings (e.g., naphthyl or anthracyl) also show intramolecular charge transfer (ICT) and greater medium sensitivity in PLA. The results involving substituent effects and ICT are supported by computational chemistry.



Cs₇Nd₁₁(SeO₃)₁₂Cl₁₆: First Noncentrosymmetric Structure among Alkaline-Metal Lanthanide Selenite Halides

Peter S. Berdonosov,* Lev Akselrud, Yurii Prots, Artem M. Abakumov, Philippe F. Smet, Dirk Poelman, Gustaaf. Van Tendeloo, and Valery A. Dolgikh

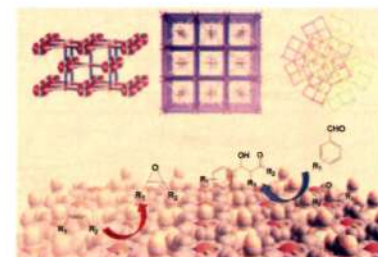
Cs₇Nd₁₁(SeO₃)₁₂Cl₁₆, the complex selenite chloride of cesium and neodymium, was synthesized in the NdOCl–SeO₂–CsCl system. The compound has been characterized using single-crystal X-ray diffraction, electron diffraction, transmission electron microscopy, luminescence spectroscopy, and second-harmonic-generation techniques. Cs₇Nd₁₁(SeO₃)₁₂Cl₁₆ crystallizes in an orthorhombic unit cell with $a = 15.911(1)$ Å, $b = 15.951(1)$ Å, and $c = 25.860(1)$ Å and a noncentrosymmetric space group $Pna2_1$ (No. 33).



Four Metalloporphyrinic Frameworks as Heterogeneous Catalysts for Selective Oxidation and Aldol Reaction

Chao Zou, Tianfu Zhang, Ming-Hua Xie, Lijun Yan, Guo-Qiang Kong, Xiu-Li Yang, An Ma,* and Chuan-De Wu*

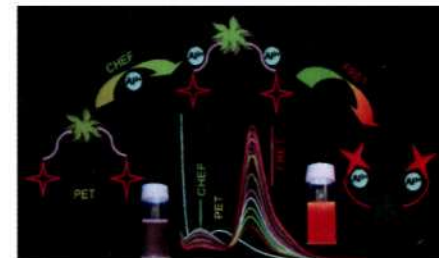
Four metalloporphyrinic frameworks present interesting framework structures that are dependent on their metal cations and have interesting catalytic properties in the selective epoxidation of olefins, oxidation of cyclohexane, and intermolecular aldol reaction of aldehydes and ketones.



Rhodamine-Based Fluorescent Probe for Al³⁺ through Time-Dependent PET–CHEF–FRET Processes and Its Cell Staining Application

Animesh Sahana, Arnab Banerjee, Sisir Lohar, Bidisha Sarkar, Subhra Kanti Mukhopadhyay, and Debasis Das*

A rhodamine-diformyl *p*-cresol-based fluorescent and colorimetric probe can sense Al³⁺ through PET–CHEF and FRET processes as established from fluorescence lifetime decay and ¹H NMR studies. The probe can detect intracellular Al³⁺ in a time-dependent manner under fluorescence microscope.



Pore Design of Two-Dimensional Coordination Polymers toward Selective Adsorption

Yuh Hijikata, Satoshi Horike, Masayuki Sugimoto, Munehiro Inukai, Tomohiro Fukushima, and Susumu Kitagawa*

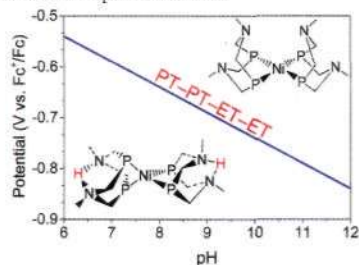
We rationally synthesized the novel series of two-dimensional assembled frameworks using four kinds of linker ligands with different lengths, and they provide different adsorption properties toward selective adsorption.



pH-Dependent Reduction Potentials and Proton-Coupled Electron Transfer Mechanisms in Hydrogen-Producing Nickel Molecular Electrocatalysts

Samantha Horvath, Laura E. Fernandez, Aaron M. Appel, and Sharon Hammes-Schiffer*

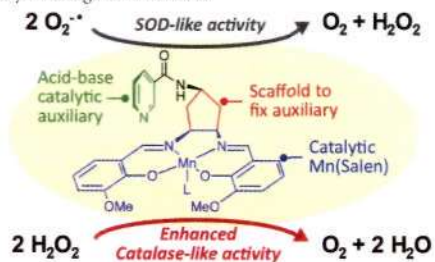
The proton-coupled electron transfer process observed in experiments with strong acid is consistent with the PT-PT-ET-ET mechanism for H₂ production. The observed slope of the pH-dependence of the reduction potential, along with calculated reduction potentials, is consistent with a two-electron/two-proton process with reduction of the doubly protonated species. The Pourbaix diagram, depicting the most thermodynamically stable species for each potential and pH, is generated from a combination of calculated and experimental data.



Manganese Salen Complexes with Acid-Base Catalytic Auxiliary: Functional Mimetics of Catalase

Yukinobu Noritake, Naoki Umezawa, Nobuki Kato, and Tsunehiko Higuchi*

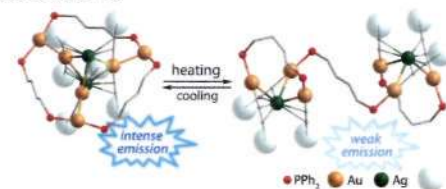
Mn(Salen) complexes exhibit both SOD- and catalase-mimetic activities. In order to enhance the catalytic activity, we designed and synthesized novel Mn(Salen) complexes with general acid-base catalytic functionality, inspired by the reaction mechanism of catalase. As expected, synthesized Mn(Salen) complexes showed superior catalase-like activity, while retaining moderate SOD-like activity. The introduced functionality did not alter the redox potential, suggesting that the auxiliary-modified complex acted as an acid-base catalyst analogous to catalase.



Sky-Blue Luminescent Au^I-Ag^I Alkynyl-Phosphine Clusters

Igor O. Koshevoy,* Antti J. Karttunen, Ilya S. Kritchenkou, Dmitrii V. Krupenya, Stanislav I. Selivanov, Alexei S. Melnikov, Sergey P. Tunik,* Matti Haukka, and Tapani A. Pakkanen

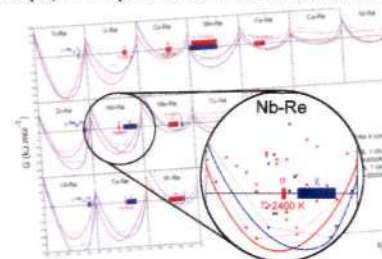
The novel Au-Ag alkynyl-phosphine complexes adopt three structural types depending on the nature of the alkynyl group. These compounds undergo unusual isomerization in solution and exhibit efficient sky-blue room-temperature phosphorescence with maximum quantum yield of 76%. The arrangement of the metal cluster framework has a crucial effect on the intensity of the luminescence observed.



χ and σ Phases in Binary Rhenium-Transition Metal Systems: a Systematic First-Principles Investigation

Jean-Claude Crivello,* Abedalhasan Breidi, and Jean-Marc Joubert

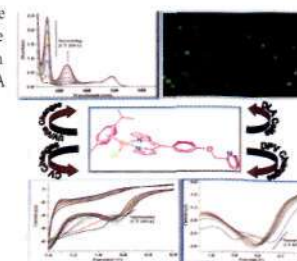
The Frank-Kasper phases, known as topologically close-packed (tcp) phases, are interesting examples of intermetallic compounds able to accommodate large homogeneity ranges by atom mixing on different sites. Among them, the χ and σ phases present two competing complex crystallographic structures, the stability of which is driven by both geometric and electronic factors. Rhenium is the element forming the largest number of binary χ and σ phases. Its central position among the transition metals in the periodic table plays an important role in the element ordering in tcp phases.



DNA Binding and Anti-Cancer Activity of Redox-Active Heteroleptic Piano-Stool Ru(II), Rh(III), and Ir(III) Complexes Containing 4-(2-Methoxyphenyl)phenyldiipyromethene

Rakesh Kumar Gupta, Rampal Pandey, Gunjan Sharma, Ritika Prasad, Biplob Koch, Saripella Srikrishna, Pei-Zhou Li, Qiang Xu, and Daya Shankar Pandey*

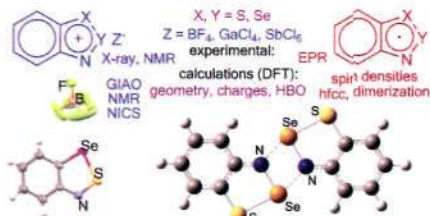
Heteroleptic "piano stool" arene complexes based on Ru(II), Rh(III), and Ir(III) have been synthesized and characterized. Antitumor activity (in vitro) of complexes have been assessed in Dalton's lymphoma (DL) ascite cell lines by trypan blue exclusion assay, acridine orange/ethidium bromide (AO/EtBr) fluorescence staining, and DNA fragmentation assay. The activity lies in the order of 2 > 1 > 4 > 3.



Experimental and Computational Study on the Structure and Properties of Herz Cations and Radicals: 1,2,3-Benzodithiazolium, 1,2,3-Benzodithiazoly, and Their Se Congeners

Alexander Yu. Makarov,* Frank Blockhuys,* Irina Yu. Bagryanskaya, Yuri V. Gatilov, Makhmut M. Shakirov, and Andrey V. Zibarev*

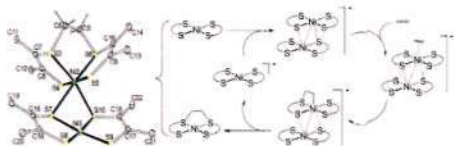
A combined experimental and computational study on the structure and properties of the archetypal Herz cations and radicals and their Se congeners was performed. These species were found to be delocalized systems featured by cyclic π -conjugation (the cations are 10π -electron aromatics). Replacement of S by Se leads to a limited perturbation of their molecular and electronic structures. Calculated dimers of the radicals in various mutual orientations appear to be unstable (with one exception) toward dissociation.



Apparent Anti-Woodward–Hoffmann Addition to a Nickel Bis(dithiolene) Complex: The Reaction Mechanism Involves Reduced, Dimetallic Intermediates

Li Dang, Mohamed F. Shibl, Xinzheng Yang, Daniel J. Harrison, Aiman Alak, Alan J. Lough, Ulrich Fekl,* Edward N. Brothers,* and Michael B. Hall*

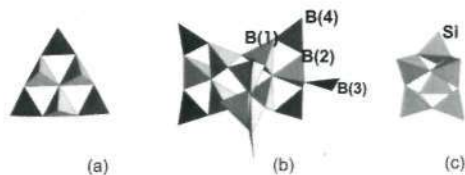
In the ligand-based reactions of Ni(tfd)₂ (tfd = S₂C₂(CF₃)₂) with alkenes, the product distribution shifts from unstable *intra*ligand adducts toward stable *inter*ligand adducts if the reduced, anionic complex [Ni(tfd)₂]⁻ is present. A combined experimental and computational study addresses the mechanism, which involves anionic dimetallic intermediates. A charge-neutral dimetallic complex, an association complex of Ni(tfd)₂ with the ethylene adduct of Ni(tfd)₂, has been crystallographically characterized.



Acentric Polyborate, Li₃[B₈O₁₂(OH)₃], with a New Type of Anionic Layer and Li Atoms in the Cavities

Elena L. Belokoneva* and Olga V. Dimitrova

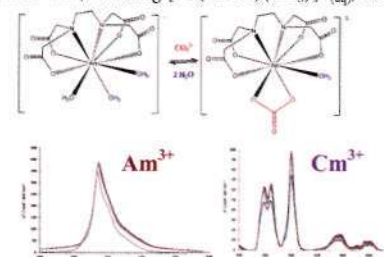
Acentric polyborate Li₃[B₈O₁₂(OH)₃] with Li atoms in the cavities has been synthesized and structurally investigated. A new type of anionic radical contains double three-membered rings (central in figure) of three hexaborate blocks (left) with the loss of three triangles, joined into the layer by additional triangle B(3). The double ring in the silicate Na₃Y[Si₆O₁₅] (right) is topologically equal to the core of the complex hexaborate ring. Both compounds, the silicate and the new borate, are proposed as fast ion conductors.



Understanding the Solution Behavior of Minor Actinides in the Presence of EDTA⁴⁻, Carbonate, and Hydroxide Ligands

Tamara L. Griffiths,* Leigh R. Martin, Peter R. Zalupski, John Rawcliffe, Mark J. Sarsfield, Nick D. M. Evans, and Clint A. Sharrad*

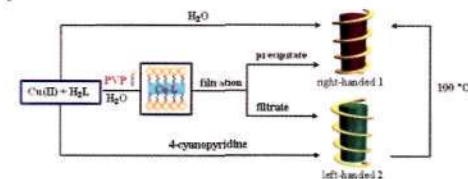
The aqueous solution behaviour of An^{III} (An = Am or Cm) in the presence of EDTA⁴⁻, carbonate and hydroxide ligands has been probed in aqueous nitrate solutions at room temperature by UV-visible absorption and luminescence spectroscopies. Ternary complexes have been shown to exist, including [An(EDTA)(CO₃)]³⁻, which form over the pH range 8 to 11.



Synthesis and Chirality Control of Bulk Crystals and Nanocrystals: From a Right-Handed Nonpolar Chain to a Left-Handed Polar Chain

Yan-Yan Yin, Yan-Li Zhao, Jian-Gong Ma,* Xiao-Chang Cao, and Peng Cheng*

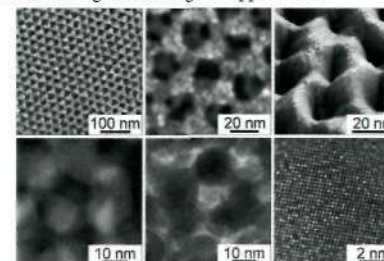
4-Cyanopyridine and poly(vinylpyrrolidone) (PVP) have been applied to control the synthesis of complexes with different helicities in bulk-crystal and nanocrystal forms, respectively, through adjustment of the number of water molecules in the crystal lattice. Conformational conversion behaviors have also been observed involving the change in symmetry between nonpolar and polar space groups.



Morphology, Microstructure, and Magnetic Properties of Ordered Large-Pore Mesoporous Cadmium Ferrite Thin Film Spin Glasses

Christian Reitz, Christian Suchowski, Venkata Sai Kiran Chakravadhanula, Igor Djerdj, Zvonko Jagličić, and Torsten Bräzesinski*

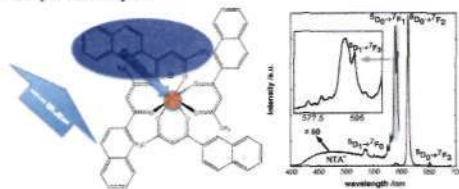
Facile polymer templating of hydrated metal nitrate salt precursors enables production of ordered mesoporous CdFe₂O₄ thin films with a cubic network of 18 nm diameter pore cavities. These materials are single phase and crystallize in the cubic spinel structure with space group *Fd3m*. Furthermore, they exhibit interesting magnetic behavior over a wide temperature range and, thus, could be particularly suitable for nanomagnetic host/guest applications.



Europium(III) Tetrakis(β -diketonate) Complex as an Ionic Liquid: A Calorimetric and Spectroscopic Study

Cláudia C. L. Pereira,* Sofia Dias, Isabel Coutinho, J. P. Leal, Luis C. Branco, and César A. T. Laia*

An intrinsic photoluminescent ionic liquid with a melting point equal to 63 °C based on europium(III) tetrakis(β -diketonate) complex with a tetraalkylphosphonium as counterion was synthesized. Calorimetric measurements show the presence of metastable liquid states upon cooling from high temperature. Eu(III) luminescence is obtained from the "antenna effect", which is characterized by spectroscopic techniques.



New Cu(I)-Ethylene Complexes Based on Tridentate Imine Ligands: Synthesis and Structure

Parisa Ebrahimpour, Mairi F. Haddow, and Duncan F. Wass*

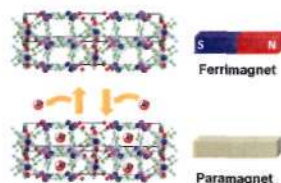
Cu(I)-ethylene complexes supported by *cis,cis*-1,3,5-(arylideneamino)cyclohexane ligands have been prepared by treatment of the ligands with CuBr and AgSbF₆ in the presence of ethylene. These complexes display reversible complexation of the ethylene molecule under mild changes to pressure, suggesting possible application in olefin separation and extraction.



Reversible Solid State Redox of an Octacyanometallate-Bridged Coordination Polymer by Electrochemical Ion Insertion/Extraction

Masashi Okubo,* Koichi Kagesawa, Yoshifumi Mizuno, Daisuke Asakura, Eiji Hosono, Tetsuichi Kudo, Haoshen Zhou,* Kotaro Fujii, Hidehiro Uekusa, Shin-ichi Nishimura, Atsuo Yamada, Atsushi Okazawa, and Norimichi Kojima*

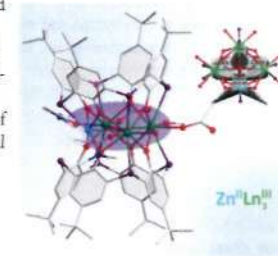
We demonstrate that the octacyanometallate-bridged coordination polymer, [Mn(H₂O)]₂[Mn(HCOO)₂/₃(H₂O)₂/₃][Mo(CN)₈]₂·H₂O, exhibits electrochemical alkali-ion insertion/extraction with high durability. Control of the valence state of Mo accompanied by ion insertion/extraction realizes a magnetic switching.



Thiacalix[4]arene-Supported Kite-Like Heterometallic Tetranuclear Zn^{II}Ln^{III} (Ln = Gd, Tb, Dy, Ho) Complexes

Kongzhao Su, Feilong Jiang, Jinjie Qian, Mingyan Wu, Kcai Xiong, Yanli Gai, and Maochun Hong*

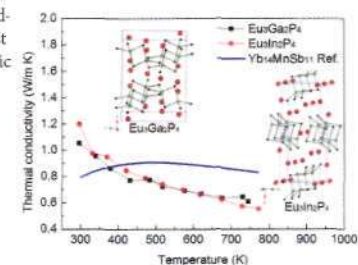
Four kite-like tetranuclear Zn^{II}Ln^{III} (Ln = Gd 1, Tb 2, Dy 3, Ho 4) clusters supported by *p*-*tert*-butylthiacalix[4]arene (H₄BTC4A) have been prepared under solvothermal conditions and structurally characterized. In the structures of complexes 1–4, each of them is capped by two tail-to-tail thiacalix[4]arene molecules and form a bent sandwich-like unit. The photoluminescent analyses indicate that luminescence sensitization of complex 2 via excitation of the H₄BTC4A ligand is efficient. The magnetic properties of complexes 1–4 are investigated, where 3 exhibits slow magnetization relaxation typical for single-molecule magnets.



Phase Characterization, Thermal Stability, High-Temperature Transport Properties, and Electronic Structure of Rare-Earth Zintl Phosphides Eu₃M₂P₄ (M = Ga, In)

Tanghong Yi, Gaigong Zhang, Naohito Tsujii, Jean-Pierre Fleurial, Alex Zevalkink, G. Jeffrey Snyder, Niels Grönbech-Jensen, and Susan M. Kauzlarich*

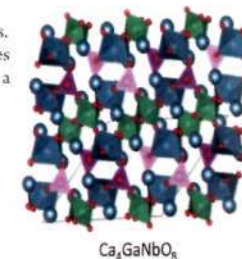
Eu₃M₂P₄ (M = Ga, In) Zintl phosphides were synthesized with a two-step solid-state method. The low thermal conductivity and high thermal stability suggest that these phosphides have potential to be good high-temperature thermoelectric materials with optimization of charge carrier concentration by appropriate extrinsic dopants.



1:1:1 Triple-Cation B-Site-Ordered and Oxygen-Deficient Perovskite Ca₄GaNbO₈: A Member of a Family of Anion-Vacancy-Based Cation-Ordered Complex Perovskites

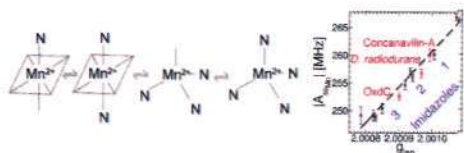
Tao Yang, John B. Claridge,* and Matthew J. Rosseinsky*

Ca₄GaNbO₈ adopts a heavily distorted oxygen-deficient perovskite structure with the rare feature of complete ordering of the three B-site cations, driven by their distinct chemistries. The anion-vacancy ordering pattern in Ca₄GaNbO₈ is driven by the coordination preferences of the three structurally distinct cations and correlated with the ordering of each cation on a distinct site.



Structure and Nature of Manganese(II) Imidazole Complexes in Frozen Aqueous Solutions

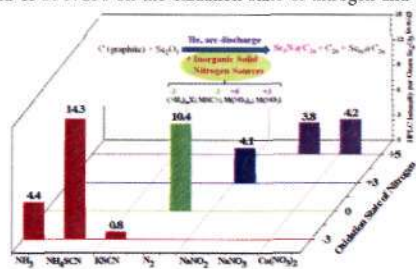
Sun Un*
The magnetic spin parameters and structures of manganese(II) imidazole complexes found in frozen aqueous solutions were determined. Both were found to be influenced by the covalency of the Mn–N bonds. The isotropic Mn^{II} hyperfine and g values were linearly correlated with the number of imidazoles. Consistent with DFT calculations, the ENDOR- and PELDOR-detected NMR spectra of frozen aqueous manganese(II) complexes with more than two imidazoles were found to have four-coordinate geometries.



A Series of Inorganic Solid Nitrogen Sources for the Synthesis of Metal Nitride Clusterfullerenes: The Dependence of Production Yield on the Oxidation State of Nitrogen and Counter Ion

Fupin Liu, Jian Guan, Tao Wei, Song Wang, Mingzhi Jiao, and Shangfeng Yang*

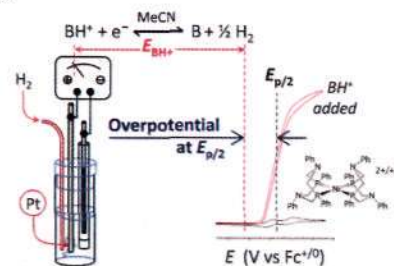
In this work, 12 nitrogen-containing inorganic compounds with variable oxidation states of nitrogen (–3 to +5) and counter ions have been successfully applied as new inorganic solid nitrogen sources toward the synthesis of Sc-NCFs, revealing the dependence of the production yield of Sc-NCFs on the oxidation state of nitrogen and counter ion.



Direct Determination of Equilibrium Potentials for Hydrogen Oxidation/Production by Open Circuit Potential Measurements in Acetonitrile

John A. S. Roberts* and R. Morris Bullock

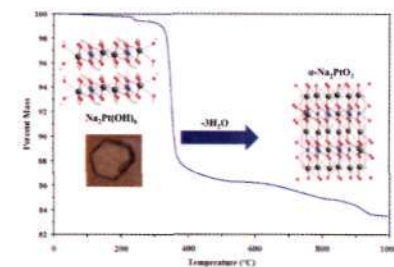
Open circuit measurements at a platinum electrode afford equilibrium potentials for a variety of acid + base solutions under 1 atm H_2 in acetonitrile. These data permit the direct measurement of overpotentials for electrocatalytic hydrogen production and oxidation mediated at a carbon electrode by homogeneous nickel bis(diphosphine) electrocatalysts. This method requires neither pK_a values, homoconjugation constants, nor an estimate for the SHE potential and thus allows direct comparison of catalytic systems in different media.



Hydroflux Crystal Growth of Platinum Group Metal Hydroxides: $Sr_6NaPd_2(OH)_{17}$, $Li_2Pt(OH)_6$, $Na_2Pt(OH)_6$, $Sr_2Pt(OH)_6$, and $Ba_2Pt(OH)_6$

Daniel E. Bugaris, Mark D. Smith, and Hans-Conrad zur Loye*

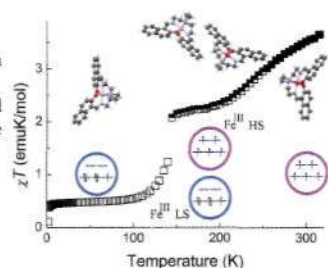
Crystals of five complex metal hydroxides containing platinum group metals were grown by a novel low-temperature hydroflux technique, a hybrid approach between the aqueous hydrothermal and the molten hydroxide flux techniques. $Sr_6NaPd_2(OH)_{17}$ (1) crystallizes in orthorhombic space group $Pbcn$ with lattice parameters $a = 19.577(4)$ Å, $b = 13.521(3)$ Å, and $c = 6.885(1)$ Å.



[Fe(η⁵-trien)]SCN, a New Two-Step Iron(III) Spin Crossover Compound, with Symmetry Breaking Spin-State Transition and an Intermediate Ordered State

Bruno J. C. Vieira, Joana T. Coutinho, Isabel C. Santos, Laura C. J. Pereira, João C. Waerenborgh, and Vasco da Gama*

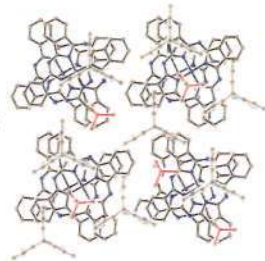
The complex [Fe^{III}(η⁵-trien)]SCN was synthesized and studied by magnetic susceptibility measurements, Mössbauer spectroscopy, and X-ray diffraction. It displays a thermally induced two-step spin crossover at 250 and 142 K, separating a high spin phase ($T > 250$ K) from an ordered intermediate phase based on the repetition of the [HS–LS] motif and a low spin phase ($T < 142$ K). The high and low spin phases are isostructural and the transitions to the intermediate phase are associated with a symmetry break.



Synthesis, Structural and Magnetic Properties of Ternary Complexes of (Me₄P⁺)[Fe(I)Pc(−2)][−]-Triptycene and (Me₄P⁺)[Fe(I)Pc(−2)][−]-(N,N,N',N'-Tetrabenzyl-*p*-phenylenediamine)_{0.5} with Iron(I) Phthalocyanine Anions

Dmitri V. Konarev,* Manabu Ishikawa, Salavat S. Khasanov, Akihiro Otsuka, Hideki Yamochi, Gunzi Saito, and Rimma N. Lyubovskaya

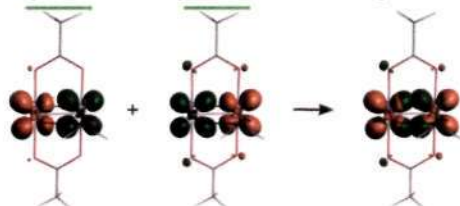
Ternary complexes (Me₄P⁺)[Fe(I)Pc(−2)][−]-TPC (1) and (Me₄P⁺)[Fe(I)Pc(−2)][−]-(TBPDA)_{0.5} (2) containing iron(I) phthalocyanine anions, tetramethylphosphonium cations, and neutral structure-forming molecules of triptycene or N,N,N',N'-tetrabenzyl-*p*-phenylenediamine have been obtained as single crystals and their crystal structures and properties have been studied. Complexes have one- and two-dimensional packing of phthalocyanine anions. The formation of coordination [Fe(I)Pc(−2)][−] dimers in both complexes evokes partial electron density transfer from the iron(I) center to the phthalocyanine macrocycle with the formation of [Fe(II)Pc(−3)][−] species.



A Theoretical Analysis of Supported Quintuple and Quadruple Chromium–Chromium Bonds

Sylvester Ndambuki and Tom Ziegler*

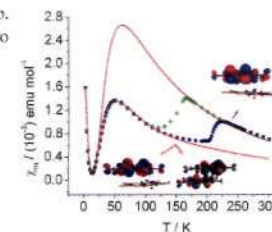
The nature of the supported and unsupported metal–metal bond in complexes of group 6 transition elements is analyzed on the basis of the extended transition state (ETS) and natural orbitals for chemical valence (NOCV) methods. The measure of the change in density corresponding to σ, π, δ -bonding components of the metal–metal bond is indicated by the deformation density plots and the corresponding deformation energy contributions. Metal–ligand contributions are also presented.



Disorder–Order Transformation and Significant Dislocation Motion Cooperating with a Surprisingly Large Hysteretic Magnetic Transition in a Nickel–Bisdithiolene Spin System

Hai-Bao Duan, Xuan-Rong Chen, Hao Yang, Xiao-Ming Ren,* Fang Xuan, and Shi-Ming Zhou*

A [Ni(mnt)₂][−] dimer compound shows magnetic bistability with a 49 K hysteresis loop. The lattice reorganization results in one type of dimer in the HT phase switching to two crystallographically different dimers in the LT phase and is responsible for the novel magnetic behavior.



Transmetalation of Chromocene by Lithium–Amide, -Phosphide, and -Arsenide Nucleophiles

Sabine Scheuermayer, Floriana Tuna, Eufemio Moreno Pineda, Michael Bodensteiner, Manfred Scheer,* and Richard A. Layfield*

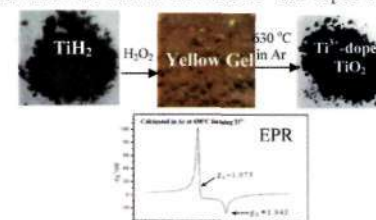
The synthesis, structure, and magnetic properties of the pnictogen-bridged compounds [(μ-η²:η²-Cp)Cr(μ-N(SiMe₃)₂Li] (1) and [(η⁵-Cp)Cr(μ-E(SiMe₃)₂)₂] (2) with E = P (2) or E = As (3), are reported. Variable-temperature magnetic susceptibility measurements on all three compounds confirmed the $S = 2$ spin configuration of the chromium(II) ions. The chromium(II) ions in the dimers 2 and 3 are strongly antiferromagnetically coupled, and modeling of the susceptibility data produced coupling constants of $J = -166$ cm^{−1} for 2 and -77.5 cm^{−1} for 3 (− J formalism).



Facile Oxidative Conversion of TiH₂ to High-Concentration Ti³⁺-Self-Doped Rutile TiO₂ with Visible-Light Photoactivity

Lauren R. Grabstanowicz, Shanmin Gao, Tao Li, Robert M. Rickard, Tijana Rajh, Di-Jia Liu, and Tao Xu*

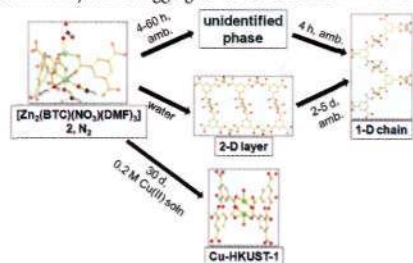
Visible-light-active Ti³⁺-self-doped rutile TiO₂ was prepared using a facile solution based oxidative method by using titanium hydride (TiH₂) as the precursor. As TiH₂ reacts with H₂O₂, the oxidant, a gel-like intermediate, is formed. Upon calcination at 630°C in Ar, a very black Ti³⁺ self-doped rutile TiO₂ is fabricated. Characterization through EPR evidently determined that a high concentration of Ti³⁺ is present within the bulk of the rutile Ti³⁺ self-doped TiO₂.



3891 **S** dx.doi.org/10.1021/ic302641v
Crystal-to-Crystal Transformations of a Series of Isostructural Metal–Organic Frameworks with Different Sizes of Ligated Solvent Molecules

Minhak Oh, Lalit Rajput, Dongwook Kim, Dohyun Moon, and Myoung Soo Lah*

Isostructural 3D metal–organic frameworks (MOFs) undergo a crystal-to-crystal transformation at ambient conditions into a 1D chain structure either directly or via different types of intermediates depending on the ligated solvent molecules and the sample handling conditions. A single crystal of the MOF with ligated DMF molecules, $[\text{Zn}_2(\text{BTC})(\text{NO}_3)(\text{DMF})_3] \cdot 2\text{N}_2$ (**2**), transforms into a single particle-like microcrystalline aggregate of Cu–HKUST-1 in a Cu^{II} -DMF solution.

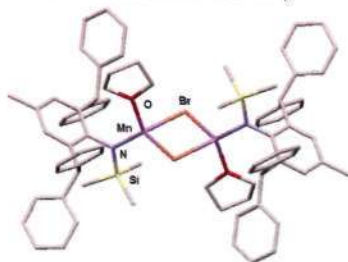


3900 **S** dx.doi.org/10.1021/ic302672a
Extremely Bulky Amido First Row Transition Metal(II) Halide Complexes: Potential Precursors to Low Coordinate Metal–Metal Bonded Systems

Jamie Hicks and Cameron Jones*

A series of extremely bulky amido first row transition metal(II) halide complexes have been prepared and structurally characterized. The majority of these are halide bridged dimers (e.g., see picture) and display distorted square-planar or tetrahedral metal coordination geometries. Two monomeric amido zinc bromide complexes are also reported, and are shown to have two- or three-coordinate metal centers, depending on the bulk of the amide ligand. The prepared complexes hold considerable potential for use as precursors to low-valent transition metal systems.

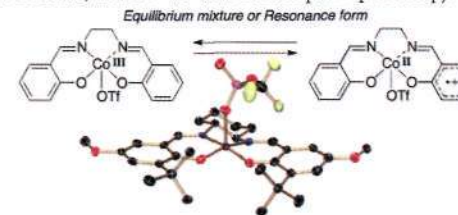
A series of extremely bulky amido first row transition metal(II) halide complexes have been prepared and structurally characterized. The majority of these are halide bridged dimers (e.g., see picture) and display distorted square-planar or tetrahedral metal coordination geometries. Two monomeric amido zinc bromide complexes are also reported, and are shown to have two- or three-coordinate metal centers, depending on the bulk of the amide ligand. The prepared complexes hold considerable potential for use as precursors to low-valent transition metal systems.



3908 **S** dx.doi.org/10.1021/ic302677f
Unique Ligand-Radical Character of an Activated Cobalt Salen Catalyst That Is Generated by Aerobic Oxidation of a Cobalt(II) Salen Complex

Takuya Kurahashi and Hiroshi Fujii*

The $\text{Co}(\text{salen})(\text{X})$ complex, which is generated by aerobic oxidation of $\text{Co}^{\text{II}}(\text{salen})$ in the presence of protic acid (HX), has been widely utilized as a versatile catalyst. The present study reveals that the $\text{Co}(\text{salen})(\text{X})$ complex ($\text{X} = \text{CF}_3\text{SO}_3^-$, SbF_6^- , and $p\text{-MeC}_6\text{H}_4\text{SO}_3^-$) contains both $\text{Co}^{\text{II}}(\text{salen}^{\bullet})(\text{X})$ and $\text{Co}^{\text{III}}(\text{salen})(\text{X})$ character, by means of X-ray crystallography, Co L-edge X-ray absorption, ^1H and ^2H NMR, and UV–vis–near-IR absorption spectroscopy.

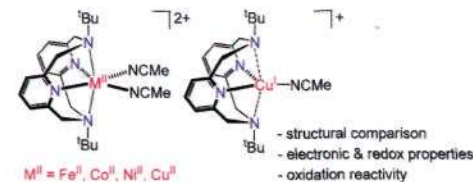


3920 **S** dx.doi.org/10.1021/ic400260z
Late First-Row Transition Metal Complexes of a Tetradentate Pyridinophane Ligand: Electronic Properties and Reactivity Implications

Julia R. Khusnutdinova, Jia Luo, Nigam P. Rath, and Liviu M. Mirica*

The synthesis and preliminary reactivity studies are reported for a series of late first-row transition metal complexes using the N,N' -di-*tert*-butyl-2,11-diaza[3.3](2,6)pyridinophane ligand ($^{\text{tBu}}\text{N}4$). These studies show that $^{\text{tBu}}\text{N}4$ is suitable to stabilize first row transition metal complexes in various oxidation states that exhibit both redox and non-redox reactivity. In addition, UV-vis and EPR studies show that $[(^{\text{tBu}}\text{N}4)\text{Fe}^{\text{II}}(\text{MeCN})_2]^{2+}$ reacts with oxidants such as H_2O_2 and peracetic acid to form high-valent Fe transient species.

The synthesis and preliminary reactivity studies are reported for a series of late first-row transition metal complexes using the N,N' -di-*tert*-butyl-2,11-diaza[3.3](2,6)pyridinophane ligand ($^{\text{tBu}}\text{N}4$). These studies show that $^{\text{tBu}}\text{N}4$ is suitable to stabilize first row transition metal complexes in various oxidation states that exhibit both redox and non-redox reactivity. In addition, UV-vis and EPR studies show that $[(^{\text{tBu}}\text{N}4)\text{Fe}^{\text{II}}(\text{MeCN})_2]^{2+}$ reacts with oxidants such as H_2O_2 and peracetic acid to form high-valent Fe transient species.

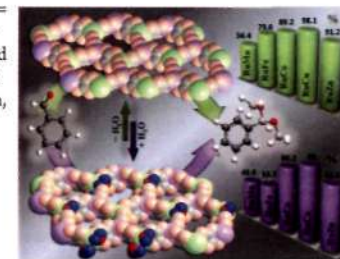


3933 **S** dx.doi.org/10.1021/ic302725v
Series of 2D Heterometallic Coordination Polymers Based on Ruthenium(III) Oxalate Building Units: Synthesis, Structure, and Catalytic and Magnetic Properties

Alla Dikhtiarenko, Sergei A. Khainakov, Imanol de Pedro, Jesús A. Blanco, José R. García,* and José Gimeno

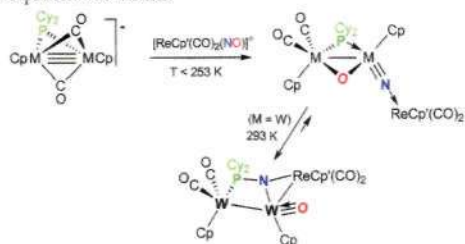
$\{[(\text{K-18-crown-6})_3][M^{\text{II}}_3(\text{H}_2\text{O})_y(\text{Ru}(\text{ox})_3)_3]\}_n$ ($M^{\text{II}} = \text{Fe}, \text{Co}, \text{Cu}, \text{Mn}, \text{Zn}; y = 0-4$) heterometallic coordination polymers have been isolated and characterized. The dehydrated compounds exhibit a reversible rehydration behavior and show higher catalytic activity in Lewis acid promoted reaction compared with the previously reported for other 2D and 3D coordination polymers. In addition, the Fe-based compound shows the existence of a cluster spin-glass-like state below 5 K.

The dehydrated compounds exhibit a reversible rehydration behavior and show higher catalytic activity in Lewis acid promoted reaction compared with the previously reported for other 2D and 3D coordination polymers. In addition, the Fe-based compound shows the existence of a cluster spin-glass-like state below 5 K.



Low-Temperature N–O Bond Cleavage and Reversible N–P Bond Formation Processes in the Reactions of the Unsaturated Anions $[M_2(\eta^5-C_5H_5)_2(\mu-PCy_2)(\mu-CO)_2]^-$ ($M = Mo, W$) with the Nitrosyl Complex $[Re(\eta^5-C_5H_5Me)(CO)_2(NO)]^+$
M. Angeles Alvarez, M. Esther García, Miguel A. Ruiz,* Adrián Toyos, and M. Fernanda Vega

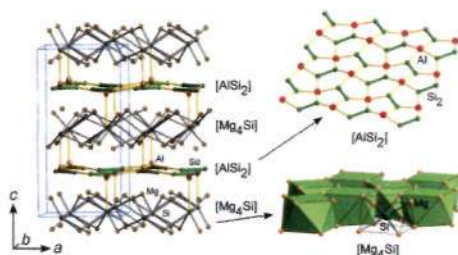
The title anions cleave the N–O bond of the nitrosyl ligand in the Re cation at 253 K to give oxo nitride derivatives, but only the tungsten complex undergoes at room temperature a further and reversible insertion of the nitride ligand into an M–PCy₂ bond, to reach equilibrium with its phosphinoimido isomer.



Structural Characterization of Magnesium-Based Compounds Mg_9Si_5 and Mg_4Si_3Al (Superconductor) Synthesized under High Pressure and High Temperature Conditions

Shidong Ji, Motoharu Imai, Haikui Zhu, and Shoji Yamanaka*

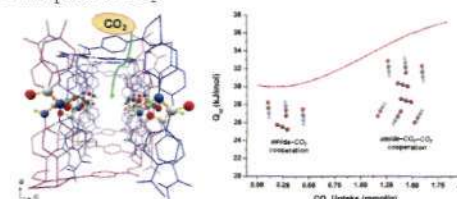
Two kinds of new Mg-based compounds Mg_9Si_5 and Mg_4AlSi_3 have been prepared under high pressure and high temperature conditions. Mg_4AlSi_3 is composed of alternate stacking of $[AlSi_2]$ and $[Mg_4Si]$ layers, which shows superconductivity with $T_c = 5.2$ K.



Cooperative Effect of Unsheltered Amide Groups on CO₂ Adsorption Inside Open-Ended Channels of a Zinc(II)–Organic Framework

Cheng-Hua Lee, Hung-Yu Huang, Yen-Hsiang Liu, Tzuoo-Tsair Luo, Gene-Hsiang Lee, Shie-Ming Peng, Jyh-Chiang Jiang, Ito Chao,* and Kuang-Lieh Lu*

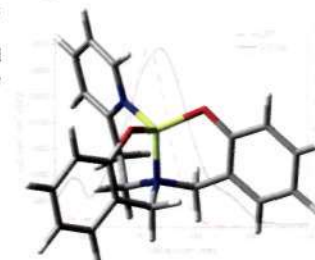
A new type of amide-containing functional MOF was prepared. It has a good adsorption selectivity for CO₂ over N₂ at low pressure and shows a specific 1:1 ratio for amide groups to adsorbed CO₂ molecules at ambient condition. The trend of isosteric heat of CO₂ adsorption (Q_{st}) reveals the existence of cooperative CO₂ adsorption. Theoretical studies suggest that the unsheltered amide groups of the open-ended channels function synergistically to provide a perfect environment for the 1:1 adsorption ratio and cooperative adsorption of CO₂.



Encapsulation of the Be^{II} Cation: Spectroscopic and Computational Study

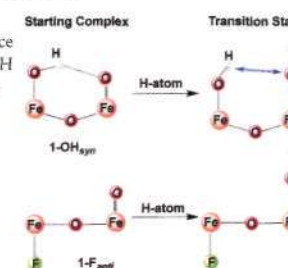
Karl J. Shaffer, Ross J. Davidson, Anthony K. Burrell, T. Mark McCleskey, and Paul G. Plieger*

The structures of a series of synthesized tetracoordinate beryllium(II) complexes with ligands derived from tertiary-substituted amines have been computationally modeled using DFT. A good correlation was observed between the calculated and the experiment spectroscopic properties. Several of the synthesized complexes gave rise to unexpected fluorescence, which could be described in terms of enhanced rigidity of certain conformations upon Be^{II} coordination.



Hydrogen-Bonding Effects on the Reactivity of $[X-Fe^{III}-O-Fe^{IV}=O]$ ($X = OH, F$) Complexes toward C–H Bond Cleavage
Genqiang Xue, Caiyun Geng, Shengfa Ye, Adam T. Fiedler, Frank Neese,* and Lawrence Que Jr.*

Complexes 1–OH and 1–F have different $(X)Fe^{III}-O-Fe^{IV}(O)$ angles due to the presence of an H-bond between the hydroxo and oxo groups of 1–OH. This difference is shown by experiment and DFT calculations to result in a significant increase in C–H bond cleavage reactivity for 1–F due to the additional activation barrier required to break its H-bond in the course of H-atom transfer to the oxoiron(IV) moiety.



3985

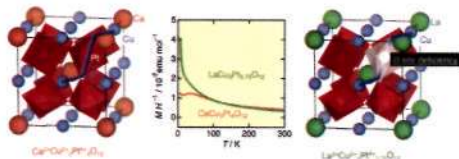
5

dx.doi.org/10.1021/ic302809v

B-Site Deficiencies in A-site-Ordered Perovskite $\text{LaCu}_3\text{Pt}_{3.75}\text{O}_{12}$

Mikiko Ochi, Ikuya Yamada,* Kenya Ohgushi, Yoshihiro Kusano, Masaichiro Mizumaki, Ryoji Takahashi, Shunsuke Yagi, Norimasa Nishiyama, Toru Inoue, and Tetsuo Irifune

An A-site-ordered perovskite $\text{LaCu}_3\text{Pt}_{3.75}\text{O}_{12}$ was synthesized at high-pressure and high-temperature of 15 GPa and 1100 °C. In $\text{LaCu}_3\text{Pt}_{3.75}\text{O}_{12}$, 1/16 of Pt ions are vacant to maintain charge balance. This is the first example of B-site cation deficiencies in an $\text{AA}'_3\text{B}_4\text{O}_{12}$ -type perovskite. Magnetic susceptibility measurements indicated a spin-glass-like behavior below $T_g = 3.7$ K in $\text{LaCu}_3\text{Pt}_{3.75}\text{O}_{12}$, which is attributed to random disturbance of the antiferromagnetic superexchange interaction by the B-site deficiencies.



3990

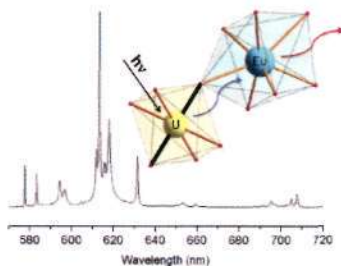
5

dx.doi.org/10.1021/ic302826u

Flux Synthesis, Crystal Structure, and Photoluminescence of a Heterometallic Uranyl-Europium Germanate with U=O–Eu Linkage: $\text{K}_6[(\text{UO}_2)\text{Eu}_2(\text{Ge}_2\text{O}_7)_2]$

Shih-Pu Liu, Meng-Ling Chen, Bor-Chen Chang,* and Kwang-Hwa Lii*

A uranyl-europium germanate has been synthesized from a KF-MoO_3 flux, and its structure contains an unusual U=O-Eu linkage. Photoluminescence studies show that, upon uranyl excitation, the energy is either transferred to the Eu^{3+} centers or lost to nonradiative processes, and the emission peaks show similar decay curves, which is fitted by a single exponential decay function with radiative lifetimes of 0.53 ± 0.03 ms.



3995

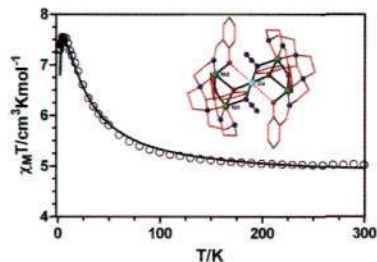
5

dx.doi.org/10.1021/ic302784q

Stepwise Formation of a Pentanuclear Ni_4Cu Heterometallic Complex Exhibiting a Vertex-Sharing Defective Double-Cubane Core and Diphenoxo- and Phenoxo/Azido Bridging Groups: A Magnetostructural and DFT Theoretical Study

Koushik Pramanik, Pijush Malpaharia, Antonio J. Mota, Enrique Colacio,* Babulal Das, F. Lloret, and Swapan K. Chandra*

The first example of a heterobridged (phenoxo/azido) pentanuclear heterometallic complex, $[\text{Ni}_4\text{Cu}(\text{L})_2(\text{N}_3)_2](\text{ClO}_4)_2$ (**1**), was prepared and magnetostructurally characterized. This compound exhibits a predominant ferromagnetic interaction with a $S = 9/2$ spin ground state.



4002

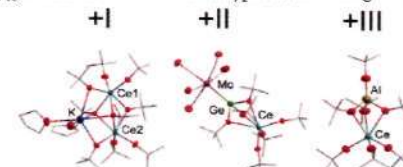
5

dx.doi.org/10.1021/ic400030j

Hetero- and Trimetallic Cerium(IV) *tert*-Butoxides with Mono-, Di-, and Trivalent Metals ($M = \text{K(I)}$, Ge(II) , Sn(II) , Pb(II) , Al(III) , Fe(III))

Johannes Schläfer, Stefan Stucky, Wieland Tyrra, and Sanjay Mathur*

A general synthetic method for the synthesis of heterobimetallic cerium(IV) *tert*-butoxides in a Lewis acid–base reaction of the appropriated homometallic alkoxides was established for mono-, di- and trivalent metal ions. The heteroleptic termetallic complexes $(\text{CO})_3\text{MoM}^{\text{II}}(\mu_2\text{-O}^t\text{Bu})_3\text{Ce}(\text{O}^t\text{Bu})_3$ ($M^{\text{II}} = \text{Ge}, \text{Sn}$) were synthesized as well as the monometallic compounds $\text{Ce}(\text{O}^t\text{Bu})_4(\text{py})_2$ and $\text{Ce}_3\text{O}(\text{O}^t\text{Bu})_{10}$ which are shown to be isotypic to the analogous derivatives of thorium and uranium.



4011

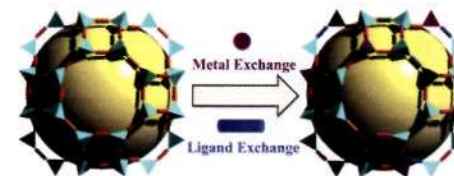
5

dx.doi.org/10.1021/ic400048g

Tandem Postsynthetic Metal Ion and Ligand Exchange in Zeolitic Imidazolate Frameworks

Honghan Fei, John F. Cahill, Kimberly A. Prather, and Seth M. Cohen*

Both ligand and metal ion exchange were achieved in a postsynthetic fashion to generate unprecedented zeolitic imidazolate frameworks (ZIFs).



4017

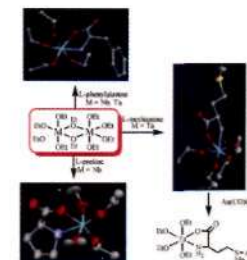
5

dx.doi.org/10.1021/ic4000654

Synthesis, X-ray Characterization, and Reactivity of α -Aminoacidato Ethoxide Complexes of Niobium(V) and Tantalum(V)

Mohammad Hayatifar, Fabio Marchetti,* Guido Pampaloni,* and Stefano Zacchini

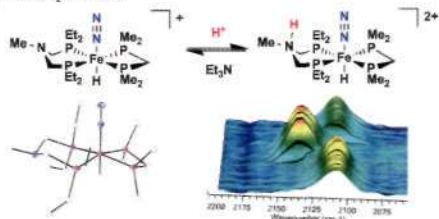
The straightforward synthesis of natural α -aminoacidato derivatives of commercial niobium(V) and tantalum(V) ethoxides has been reported. The first examples of crystallographically characterized coordination adducts of such metals bearing an aminoacidato ligand are provided.



Protonation of Ferrous Dinitrogen Complexes Containing a Diphosphine Ligand with a Pendent Amine

Zachariah M. Heiden, Shentan Chen, Michael T. Mock,^{*} William G. Dougherty, W. Scott Kassel, Roger Rousseau, and R. Morris Bullock

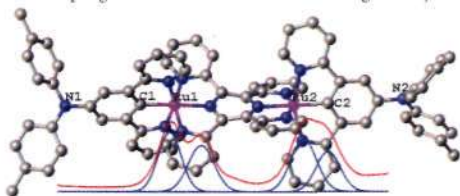
The addition of acids to ferrous dinitrogen complexes $[\text{FeX}(\text{N}_2)(\text{P}^{\text{Et}}\text{N}^{\text{Me}}\text{P}^{\text{Et}})(\text{dmpm})]^+$ ($\text{X} = \text{H}, \text{Cl}, \text{or Br}; \text{P}^{\text{Et}}\text{N}^{\text{Me}}\text{P}^{\text{Et}} = \text{Et}_2\text{PCH}_2\text{N}(\text{Me})\text{CH}_2\text{PEt}_2$; and $\text{dmpm} = \text{Me}_2\text{PCH}_2\text{PMe}_2$) gives protonation at the pendent amine of the diphosphine ligand rather than at the dinitrogen ligand. This protonation increased the ν_{N_2} band of the complex by 25 cm^{-1} and shifted the $\text{Fe}(\text{II}/\text{I})$ couple by 0.33 V to a more positive potential.



Multi-Center Redox-Active System: Amine–Amine Electronic Coupling through a Cyclometalated Bisruthenium Segment

Chang-Jiang Yao, Yu-Wu Zhong,^{*} and Jiannian Yao

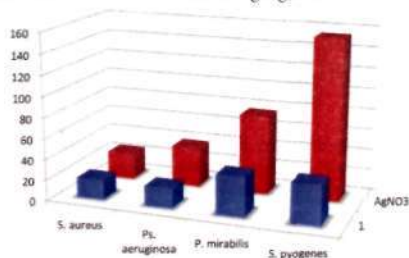
A multicenter redox-active system with a linear $\text{N}-\text{Ru}-\text{Ru}-\text{N}$ array has been synthesized and characterized with single-crystal X-ray analysis. This system displays four consecutive and separate anodic redox waves at low potentials, indicating the presence of amine–amine electronic coupling with a distance of 19.16 \AA through the cyclometalated bisruthenium segment.



Effects of Different Substituents on the Crystal Structures and Antimicrobial Activities of Six Ag(I) Quinoline Compounds

Alshima'a A. Massoud,^{*} Vratislav Langer, Yousry M. Gohar, Morsy A. M. Abu-Youssef, Janne Jänis, Gabriella Lindberg, Karl Hansson, and Lars Öhrström^{*}

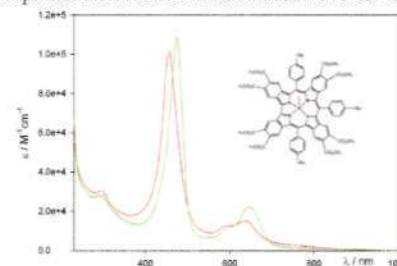
$[\text{Ag}(\text{5-nitroquinoline})_2]\text{NO}_3$ (**1**) performed significantly better than AgNO_3 in an MIC test against four standard bacterial strains. The investigation of this series of Ag(I) quinoline compounds (**1–6**) is complemented by X-ray diffraction and solution studies, as well as testing on clinically isolated multidrug-resistant strains. The role of intermolecular interactions in determining the Ag(I) coordination number in the solid state is highlighted.



Aluminum, Gallium, Germanium, Copper, and Phosphorus Complexes of meso-Triaryltetrabenzocorrole

Giuseppe Pomarico, Sara Nardis, Mario L. Naitana, M. Graça H. Vicente, Karl M. Kadish,^{*} Ping Chen, Luca Prodi, Damiano Genovese, and Roberto Paolesse^{*}

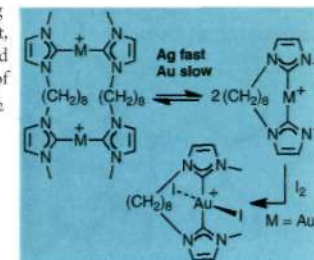
The definition of a synthetic route to the 5,10,15-triaryltetrabenzocorrole free base opens a way to the preparation of the corresponding metal complexes. The influence of the π -aromatic system on the corrole properties is studied in detail by photophysical, electrochemical, and spectroelectrochemical characterization of these functionalized corroles.



Mono- and Dinuclear Ag(I), Au(I), and Au(III) Metallamacrocycles Containing N-Heterocyclic Dicarbene Ligands

Juan Gil-Rubio,^{*} Verónica Cámara, Delia Bautista, and José Vicente^{*}

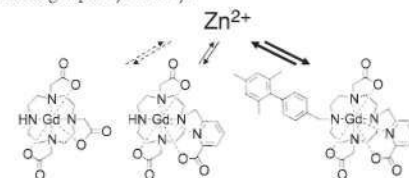
The exchange between Ag(I) mono- and dinuclear metallamacrocycles containing dicarbene ligands is rapid at room temperature, in the NMR time scale. In contrast, their Au(I) analogues exchange slowly. In these equilibria, which are here reported for the first time, the mononuclear/dinuclear ratio depends mainly on the length of the $(\text{CH}_2)_n$ linker. Oxidation of one of the mononuclear Au(I) complexes with I_2 gives an unprecedented type of Au(III) complex.



Is Macrocyclic a Synonym for Kinetic Inertness in Gd(III) Complexes? Effect of Coordinating and Noncoordinating Substituents on Inertness and Relativity of Gd(III) Chelates with DO3A-like Ligands

Miloslav Polasek and Peter Caravan^{*}

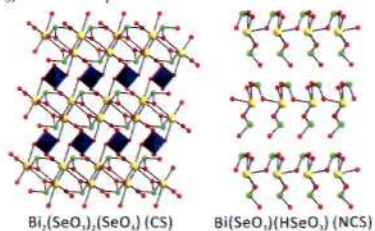
Macrocyclic DO3A-like ligands with one acetate moiety replaced with bidentate (methyl picolinate or ethoxyacetate) or bulky monodentate (methyl phosphonate) donor arm provided monohydrated gadolinium(III) complexes. The water residency times spanned 2 orders of magnitude from very fast (ns) to very slow (ms) exchange regimes. Despite coordination of all donor atoms, these complexes showed surprisingly low kinetic inertness that was further decreased upon alkylation of a secondary amine with a noncoordinating biphenyl moiety.



New Bismuth Selenium Oxides: Syntheses, Structures, and Characterizations of Centrosymmetric $\text{Bi}_2(\text{SeO}_3)_2(\text{SeO}_4)$ and $\text{Bi}_2(\text{TeO}_3)_2(\text{SeO}_4)$ and Noncentrosymmetric $\text{Bi}(\text{SeO}_3)(\text{HSeO}_3)$

Eun Pyo Lee, Seung Yoon Song, Dong Woo Lee, and Kang Min Ok*

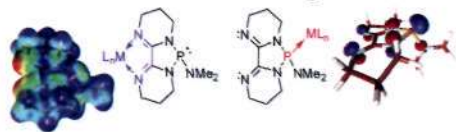
Three new bismuth selenium oxides, $\text{Bi}_2(\text{SeO}_3)_2(\text{SeO}_4)$, $\text{Bi}_2(\text{TeO}_3)_2(\text{SeO}_4)$, and $\text{Bi}(\text{SeO}_3)(\text{HSeO}_3)$ have been successfully synthesized. Centrosymmetric $\text{Bi}_2(\text{SeO}_3)_2(\text{SeO}_4)$ and $\text{Bi}_2(\text{TeO}_3)_2(\text{SeO}_4)$ exhibit three-dimensional framework structures, and noncentrosymmetric $\text{Bi}(\text{SeO}_3)(\text{HSeO}_3)$ shows a layered structure.



Conformationally Constrained N-Heterocyclic Phosphine–Diimine with Dual Functionality

Georgios Mourgas, Martin Nieger, Daniela Förster, and Dietrich Gudat*

An N-heterocyclic phosphine–diimine with a tricyclic molecular skeleton acts as ambident ligand which provides dual functionality: metal centers bind through the P-donor site if the interaction is orbital controlled and at the diimine unit if the interaction is charge controlled. Attachment of a metal center at either position deactivates the remote coordination site.



High Quantum Yield Molecular Bromine Photoelimination from Mononuclear Platinum(IV) Complexes

Alice Raphael Karikachery, Han Baek Lee, Mehdi Masjedi, Andreas Ross, Morgan A. Moody, Xiaochen Cai, Megan Chui, Carl D. Hoff,* and Paul R. Sharp*

High quantum yield bromine photoeliminations from *trans*-Pt(PEt₃)₂(R)(Br)₃ are endothermic and endergonic with free energies from 2.2 to 21.8 kcal/mol. Solution trapping experiments suggest a radical-like excited state precursor to bromine elimination.

